Supporting Information for

# Controlling fluorescence emission with split-ring-resonator-based plasmonic metasurfaces

*Si Luo, Qiang Li[*], Yuanqing Yang, Xingxing Chen, Wei Wang, Yurui Qu, and Min Qiu*

State Key Laboratory of Modern Optical Instrumentation, College of Optical Science and Engineering, Zhejiang University, Hangzhou 310027, China,

**The Supporting Information includes the following contents:**

**I. The experimental setup to characterize the fluorescence properties**

**II. Mode analysis at different incident angles**

**III. Fundamental magnetic resonance at x-polarized incidence**

**IV. The absorbance and emission spectra of Rh 800.**

**V. Fluorescence enhancement factors compared with the calculated electric field enhancements.**

## I. The experimental setup to characterize the fluorescence properties

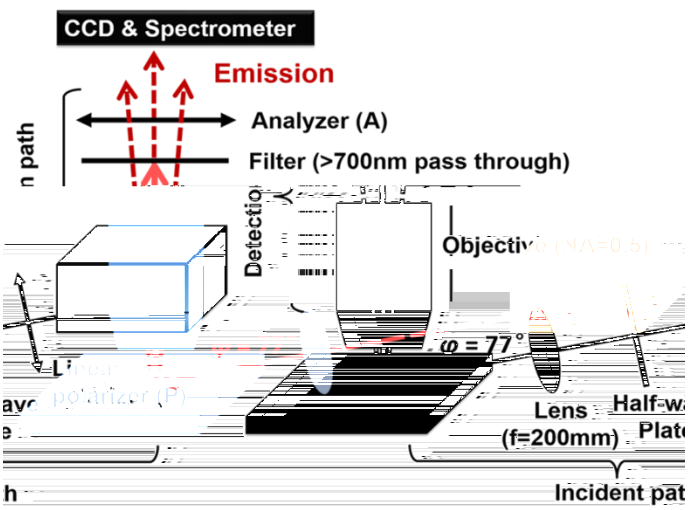

**Figure S1.** A schematic diagram depicting the control over the fluorescence emission with the SRR-based plasmonic metasurface

## II. Mode analysis at different incident angles

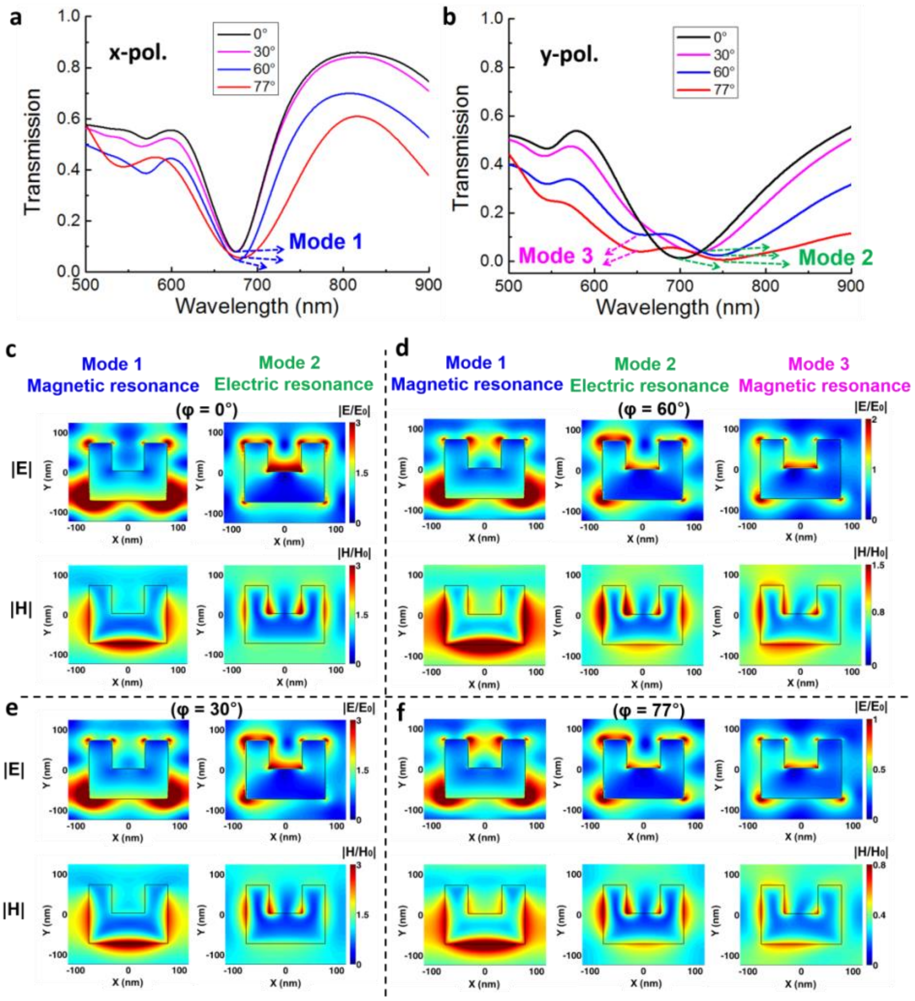


**Figure S2. (a, b)** Simulated transmission spectra of the SRR based metasurface at x-polarized and y-polarized incidence. The spectra at different incident angles of $\varphi$ = 0° (black), $\varphi$ = 30° (pink), $\varphi$ = 60° (blue) and $\varphi$ =77° (red) are denoted. Three resonant modes are marked. **(c-e)** Simulated electric and magnetic field intensity distributions of the corresponding resonant modes at different incident angles of **(c)** $\varphi$ = 0°, **(d)** $\varphi$ = 30°, **(e)** $\varphi$ = 60° and **(f)** $\varphi$ = 77°.

For x-polarized incidence, the resonant wavelength of the magnetic mode (Mode 1) remains almost unchanged with incident angles $\varphi$ varying from 0° to 77° (Fig. S2a). The electric and magnetic field distributions of Mode 1 are also similar at different incident angles $\varphi$ (Fig. S2c-f).

For y-polarized incidence, the resonant wavelength of the electric mode (Mode 2) is red-shifted with increasing incident angles $\varphi$ (Fig. S2b). A new magnetic mode (Mode 3) emerges with similar electric and magnetic field distributions at 60° and 77° oblique incidence.

## III. Fundamental magnetic resonance at x-polarized incidence

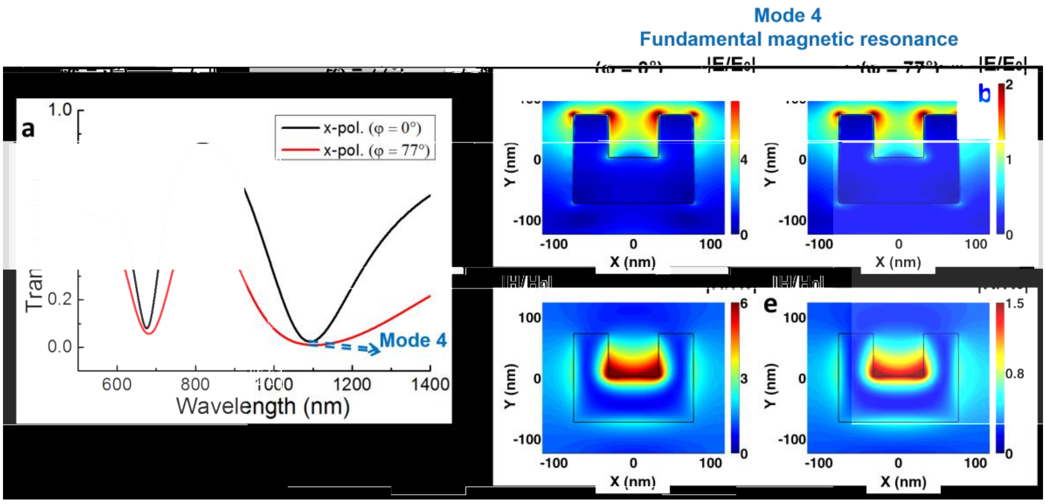


**Figure S3. (a)** Simulated transmission spectra of the SRR based metasurface at x-polarized incidence. The black and red lines denote the incident angles of $\varphi$ = 0° and $\varphi$ = 77°, respectively. The fundamental magnetic modes (Mode 4) at around 1100 nm are marked with arrows. **(b, d)** Simulated electric **(b)** and magnetic **(d)** field intensity distributions of Mode 4 at normal incidence ($\varphi$ = 0°) **(c, e)** Simulated electric **(c)** and magnetic **(e)** field intensity distributions of Mode 4 at oblique incidence ($\varphi$ = 77°).

## IV. The absorbance and emission spectra of Rh 800.

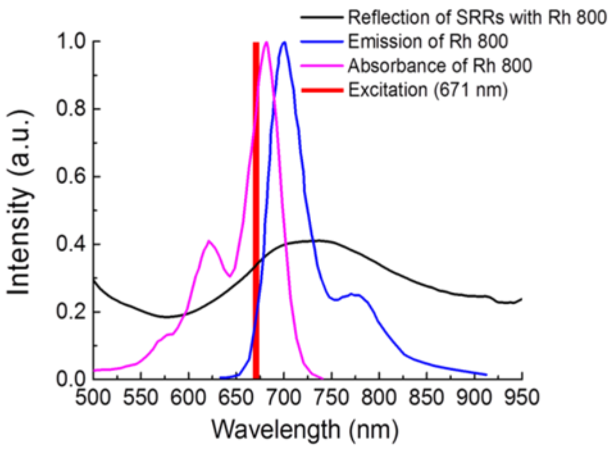

**Figure S4.** The resonance (the reflection of the SRR-based metasurface with dyed PVA film) is plotted with the absorption and emission spectra of the dye. (The absorbance and emission spectra data are adopted from Ref. [53].)

[53] A. Alessi, M. Salvalaggio, and G. Ruzzon, *J. Lumin.* **134,** 385–389 (2013).

## V. Fluorescence enhancement factors compared with the calculated electric field enhancements.

**Table S1**. Calculated field enhancement factor and experimental fluorescence enhancement factor at 77° oblique incidence.

| Incident Polarization | $\left(\frac{E}{E_0}\right)^2_{671}$ (Cal.) | $\left(\frac{E}{E_0}\right)^2_{706}$ (Cal.) | $\left(\frac{E}{E_0}\right)^2_{671}\left(\frac{E}{E_0}\right)^2_{706}$ (Cal.) | EF (Exp.) |
|---|---|---|---|---|
| x-pol. | 5.73 | 5.19 | 29.74 | 18 |
| y-pol. | 2.80 | 3.46 | 9.69 | 8 |

**Table S2**. Calculated field enhancement factor and experimental fluorescence enhancement factor with the cross-section schematics of two side arms coated with different thickness of PVA shown in the insets.

| | Case I | Case II | Case III |
|---|---|---|---|
| Incident Polarization | $\left(\frac{E}{E_0}\right)^2_{671}\left(\frac{E}{E_0}\right)^2_{706}$ (sim.)<br>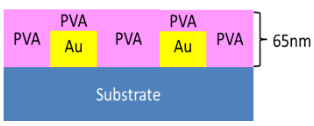<br> | EF (exp.)<br>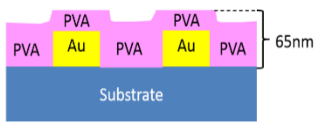<br> | $\left(\frac{E}{E_0}\right)^2_{671}\left(\frac{E}{E_0}\right)^2_{706}$ (sim.)<br>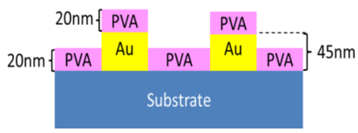<br> |
| x-pol. | 29.74 | 18 | 14.20 |
| y-pol. | 9.69 | 8 | 4.64 |

*The measured thickness of the gold film and the spin-coated PVA film is 45 nm and 20 nm, respectively.